WESTERN REGION TECHNICAL ATTACHMENT
NO. 97-39
DECEMBER 23, 1997

THE SEVERE WEATHER EVENT OF 18 JUNE 1997: AN EXAMPLE OF SPLITTING SUPERCELLS

Randall Graham - NWSFO Salt Lake City, UT
and
Mike Staudenmaier, Jr. - NWSO Flagstaff
(Formerly NWSFO SLC/ WRH-SSD)

Introduction

The most organized type of thunderstorm is the supercell, which is responsible for much of the summertime storm damage occurring in the United States. While supercells form a small fraction of the total number of severe thunderstorm events, they tend to be responsible for a rather large fraction of damage associated with severe thunderstorms. Supercells are associated with particular environmental shear characteristics, making the hodograph the best diagnostic tool to determine possible storm type. When the hodograph is essentially a straight line (Fig. 1), the development of splitting supercells is favored. This Technical Attachment (TA) will discuss the theory behind splitting supercells, and then discuss and investigate the severe weather event of 18 June 1997 in southeast Idaho, which was a classic example of this type of storm.

The Theory Behind Splitting Supercells

Forecasters have known for some time that supercells tend to be deviant movers, that is, they generally move in a direction other than along the mean shear vector (surface - 6 km depth). In the Northern Hemisphere, supercells tend to move to the right of the mean shear vector, and tend to move slower than the magnitude of the vector would suggest. Numerical work by Wilhelmson and Klemp (1978), Klemp and Wilhelmson (1978), and Weisman and Klemp (1982) have helped forecasters understand the dependence of supercells on vertical wind shear and buoyancy. Their results suggest a spectrum of storm types ranging from short-lived single cells, through multicellular thunderstorms, to the longer-lived supercell. It was found that the environmental wind shear associated with the storm environment combined with the amount of buoyancy in the atmosphere determined the type of storms which will most likely occur. Of particular interest for this TA, is the

concept of splitting supercells and what storm environment supports this type of phenomena.

Using one dimensional wind profiles, Klemp and Wilhelmson (1978) found that the tendency of an initial storm to split into two self-sustaining storms was strongly dependent on the intensity and distribution of the low-level wind shear. When the hodograph is more or less a straight line, the most likely development due to this shear profile is splitting storms that form mirror images of one another. In this environment, neither of the pair is favored, so both storms tend to persist. When splitting occurs, a cyclonically rotating updraft propagates to the right of the mean wind, while an anticyclonically rotating one moves to the left. However, Klemp and Wilhelmson (1978) along with Weisman and Klemp (1982) suggest that when the lowest several kilometers of the hodograph are curved, one member of the split pair is favored over the other. This means that the favored one persists while the unfavored one dies out rapidly, if it even forms. It turns out that a clockwise turning of the hodograph favors the cyclonic, right-moving member of the split, while counterclockwise turning favors the anticyclonic, left-moving member (in the Northern Hemisphere). The sort of storm most typical, and which has been seen most often by forecasters, is a cyclonically-rotating, right-moving storm; this sort of storm becomes likely when the hodograph's lowest several kilometers are characterized by clockwise turning of the hodograph. In this situation, the left-mover never forms, or if it does, quickly dies away, leaving just the right-mover to continue. This hodograph curvature arises from both dynamical and frictional effects. In the Northern Hemisphere, the Ekman Spiral dictates that, because of frictional effects, the wind generally will veer with height through the boundary layer, creating a clock-wise turning of the lower atmosphere. This also favors right-moving supercells.

How the rotation develops in splitting cells has been widely debated. The most widely accepted theory was discussed by Wilhelmson and Klemp (1978). As shown in Figure 2a, during the initial stages of updraft development, there is a tilting of the vorticity associated with the mean shear flow, which gives rise to a vortex pair straddling the updraft. Due to the updraft tilting this mean shear flow, there is cyclonic rotation on the southern flank of the storm and anticyclonic rotation on the northern flank (for a storm moving to the east). Waterloading in the updraft which creates a downdraft (Wilhelmson and Klemp 1978), along with forced ascent along the gust front (Brown 1992) and lifting of low-level air by the mid-level vortices along the storms flanks through dynamical vertical pressure gradients (Rotunno and Klemp 1982) all act to split the original pair of vortices into two separate pairs (Fig. 2b). The lifting of low-level air by the mid-level vortices was found to be a significant contributor to storm splitting, and can even cause storm splitting without precipitation and the associated downdraft (Rotunno and Klemp 1982). This was verified by observations of splitting towers occurring without any observable precipitation by Bluestein et al. (1990). Thus, the right-moving storm has a cyclonically rotating updraft and an anticyclonically rotating downdraft, while the opposite is true for the left-mover. These new updrafts strengthen the vorticity further through stretching, which in turn enhances the dynamic vertical pressure gradients.

By this time, the downdraft of the original storm has produced a cool outflow boundary which is moving away from the thunderstorms. For the cyclonically-rotating right-moving storm, the downdraft is located along the rear and left flank, and outflow near the ground spreads out underneath the updraft, forcing continuous uplifting of the moist low-level inflow along the right flank (Klemp and Wilhelmson 1978). In this manner, the storm maintains its moisture source and tends to propagate to the right. Remember that storm movement is the sum of two contributions: advection and propagation. Thus, even though the advection term is along the mean shear vector, the propagation term is to the right of the storm. Therefore, the actual storm movement is to the right of the mean shear vector. For the anticyclonically-rotating left-moving system, the convergence would be along the left portion of the outflow boundary, creating a storm movement to the left of the mean shear vector. This deviant propagation alters the storm-relative helicity values and may encourage supercell development (Vasiloff et al. 1984).

If the low, middle, and upper-level winds lie along a one-directional shear line, i.e. a straight line hodograph, both right- and left-moving storms formed through splitting will have similar opportunities to establish a self-sustaining structure. However, in the real world, and especially in the western United States, topography and influences from nearby storms can modify the storm environment and cause one storm or another to be preferred, even with straight line hodographs. Curvature of the wind hodograph causes a relative enhancement of the downdraft associated with one of the storms, which in turn increases the gustfront-induced convergence beneath the storm. Thus, with a hodograph that turns clockwise with height, development of the right-moving storm is favored, while if it turns counterclockwise, the left-moving storm is favored.

Documentation of the most organized types of severe weather (splitting cells, supercells, bow echoes, etc.) remains somewhat limited across much of the western United States. However, the recent installation of WSR-88D's in many locations across the West is resulting in increasing documentation of such events. The following section will discuss the 18 June 1997 event, examining both the hodograph and the WSR-88D output. This case is an excellent example of splitting supercells which can occur in Western Region.

The Synoptic Scale Environment

At 1200 UTC a broad flat ridge of high pressure was in place over the western United States with a weak mid-level shortwave moving across the northern Intermountain Region. A west-to-east oriented jet streak with core speeds in excess of 60 knots was located over southern Idaho. An area of low pressure was located in southwest Manitoba with an associated surface trough that extended from northwest Montana through southeast Idaho. A relatively strong area of high pressure at the surface was located just off of the northwest Oregon coast. Surface temperatures at 1800 UTC ranged from the low to mid 70s (F) in southeast Idaho to near 90 (F) in east central Utah. A pocket of low-level moisture was located across northwest Utah and northeast Nevada extending into southeast Idaho. Dewpoint temperatures were in the mid to upper 50s across this area, while dewpoints

across the remainder of the Great Basin were generally in the mid 30s to mid 40s. Synoptic-scale motions associated with the shortwave were likely rather weak with some enhancement due to the low static stability and low-level convergence along the surface trough.

Soundings and Hodographs

An examination of the morning RAOBS and hodographs from Salt Lake City, UT and Boise, ID clearly showed an environment favorable for the development of splitting cells. The Salt Lake City, UT 1200 UTC upper-air sounding (not shown) exhibited nearly unidirectional flow from the west-southwest above 850 mb. Below 850 mb, the Salt Lake City sounding indicated south-southeast winds. It should be noted that due to the orientation of the Snake River Valley (Fig. 3) in southern Idaho (the region where the splitting cells developed) afternoon southwesterly low-level flow is favored. Strong speed shear was evident in the Boise, ID sounding with speeds of 5 knots near the surface increasing to near 55 knots at 300 mb. The hodograph from the Salt Lake City sounding (Fig. 4) exhibited nearly unidirectional shear above 850 mb which is favorable for the development of splitting cells. With the expected southwest low-level winds due to flow channeling across the eastern portion of the Snake River Plain, as previously mentioned, one could assume nearly unidirectional shear through the entire profile. In fact, surface observations from Pocatello, ID (roughly 25 miles from the location where the initial development of the cell occurred) indicated afternoon winds between 210-230 degrees at 6-15 knots which helped confirm the above assumption.

The Event

Thunderstorms developed along the surface boundary by 1830 UTC. The initial development of the cell that led to the split occurred around 1920 UTC about 25 miles southwest of Pocatello, ID. Cells were moving with the mean flow in the storm-bearing layer from about 265 degrees at 20 knots. The first evidence that a split was occurring in this cell was noted in the 1940 UTC scan as a new updraft became apparent on the cell's left flank where additional returns appeared in the mid-levels of the storm. By 1955 UTC, the split became more evident as a notch appeared on the western extent of the low-level echo. At this point two separate centers of rotation were noted in the storm-relative velocity product indicating the existence of two separate updrafts, one rotating cyclonically (right moving storm), and the other anti-cyclonically (left moving storm). The 0.5 degree elevation scan from the Salt Lake City, UT WSR-88D (KMTX), which was located 80 nm south of the storms, was interrogating the storms at approximately 15,500 feet above radar level. The radar is located at 6460 feet MSL while the valleys in southern Idaho are around 4500 feet MSL. This means that the lowest elevation scan was hitting the cells around 17,000 feet AGL. Based on the morning soundings at Salt Lake City and Boise cloud bases were expected to be in the neighborhood of 10,000 AGL. Therefore, the KMTX radar was not sampling the lowest 6,000-7,000 feet of the storm.

By 1959 UTC, the cells had clearly separated (Fig. 5). At this point in time, the right moving storm appeared to be significantly stronger than the left moving storm. The right member was exhibiting 3 to 4 nm of overhang and a displacement of the echo top over the tight low-level reflectivity gradient on the south side of the storm (Fig. 6). Cyclonic rotation was noted in the storm in the 0.5 degree elevation scan of the KMTX WSR-88D. At this time, spotter reports from the town of Grace, ID indicated that one and one-half inch diameter hail was being generated by this cell. There were also funnel clouds reported in Grace at this time.

Of note in the 2004 UTC scan was the evidence of an anticyclonically rotating downdraft in the right moving cell and a cyclonically rotating downdraft in the left moving cell (Fig. 7). This fits the conceptual models put forth by Weisman and Klemp of a pair of vorticity couplets that appeared in model simulations of splitting cells. These storms also tended to follow the Weisman/Klemp findings regarding storm motion. During this case, the left moving storm was the more deviant of the two cells with a greater angle between it and the mean wind vector along with a faster forward movement, which was 50 percent greater than the mean wind. This is important because the storm-relative velocity algorithm was subtracting out an average storm motion of 260 degrees at 21 knots from the base velocity product. Due to the deviant motion of the split cells, this value was not the correct value to use to assess rotation in these two cells. The right mover was moving from 280 degrees at 20 knots, while the left mover was moving from 245 degrees at 30 knots. Using an incorrect value of storm motion resulted in there being less inbound velocity, particularly with the left moving storm. If this is taken into consideration, a more balanced rotation signature would be seen with the left mover.

For the next 15 minutes, the right-moving storm continued to exhibit significant mid-level overhang and moderate cyclonic rotation. The left-moving storm, while it exhibited moderate values of anticyclonic rotation and a tight low-level reflectivity gradient, showed little in the way of overhang. At 2014 UTC, the VR-Shear function yielded a value of 31 knots for the cyclonic circulation and 26 knots for the anticyclonic rotation. The depth of the cyclonic circulation was approximately 16,000 feet while the anticyclonic circulation was approximately 10,000 feet deep. This did not account for the 6,000 feet of echo that was below the 0.5 degree elevation scan. Calculations using these depth and strength values classify these rotation couplets as minimal to moderate mesocyclones. Additional funnel cloud reports continued to be received for the southern cell through this time.

As the cells continued through their life cycle, they developed into more of a classic mirror image as seen in the model simulations of splitting cells (Fig. 8). The cells exhibited opposite rotations in the relative storm velocity panels through much of their existence. The right moving storm exhibited deep rotation (10,000 feet or greater) from 1959 UTC until approximately 2044 UTC, while the left moving storm contained deep rotation from approximately 2009 UTC until 2059 UTC. The cells moved to near the Idaho/Wyoming border before finally dissipating around 2130 UTC. The cells spent most of their life cycle over sparsely populated regions of southeast Idaho, and no additional reports of severe weather were received after the cells moved through Grace, ID, although it is quite possible that severe weather existed with these cells until they began weaken after 2040 UTC.

Conclusions

Documentation of the most organized types of severe weather (splitting cells, supercells, bow echoes, etc.) remains somewhat limited across much of the western United States. This TA presented a review of the fundamentals of the processes that lead to splitting cells and then examined a split that occurred in southeast Idaho on 18 June 1997. The radar signatures and life cycle of the cells were similar to those of splitting cells that occur in the Midwest, as well as to model simulations. This case study highlights the forecaster's need to anticipate the type of convection by examining the hodographs and upper-air soundings in the pre-storm environment for the area of concern. By anticipating ahead of time the type of convection that will occur, radar operators will be much better prepared to handle severe weather when it does develop. This TA also demonstrates that the forecaster must be aware of how to most effectively interpret the storm-relative velocity product. The numerous WSR-88D radars implemented across the western United States will undoubtedly lead to more frequent documentation of severe storms, ultimately leading to a better understanding of severe weather phenomena in the western United States.

References

Bluestein, H.B., E.W. McCaul, Jr., G.P. Byrd, R.L. Walko, and R.P. Davies-Jones, 1990: An observational study of splitting convective clouds. *Mon. Wea. Rev.*, **118**, 1359-1370.

Brown, R.A., 1992: Initiation and evolution of updraft rotation within an incipient supercell thunderstorm. *J. Atmos. Sci.*, **49**, 1997-2014.

Klemp, J.B. and R.B. Wilhelmson, 1978: Simulations of right- and left-moving storms produced through storm splitting. *J. Atmos. Sci.*, **35**, 1097-1110.

Vasiloff, S. V., E. A. Brandes, R. P. Davies-Jones, and P. S. Ray, 1986: An investigation of the transition from multicell to supercell storms. *J. Climate and Appl. Meteor.,* **25**, 1022-1036.

Weisman, M.L., and J.B. Klemp, 1982: The dependence of numerically simulated convective storms on vertical wind shear and buoyancy. *Mon. Wea. Rev.*, **110**, 504-520.

Wilhelmson, R.B. and J.B. Klemp, 1978: A numerical study of storm splitting that leads to long-lived storms. *J. Atmos. Sci.*, **35**, 1974-1985.

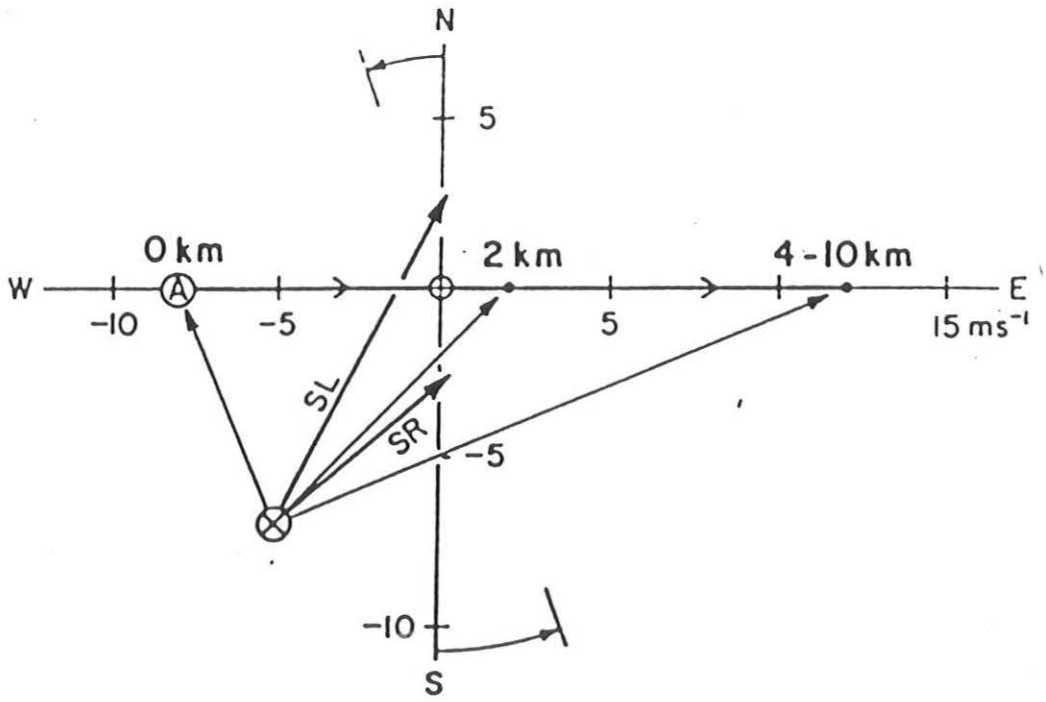

Figure 1 Wind hodograph depicting unidirectional environmental shear. The thin arrows represent the 0, 2, and 4 km wind vectors relative to a fixed ground based origin (circles with x in center). Heavy arrows (SR and SL) show the propagation of right and left moving storms, respectively. (Figure taken from Klemp and Wilhelmson)

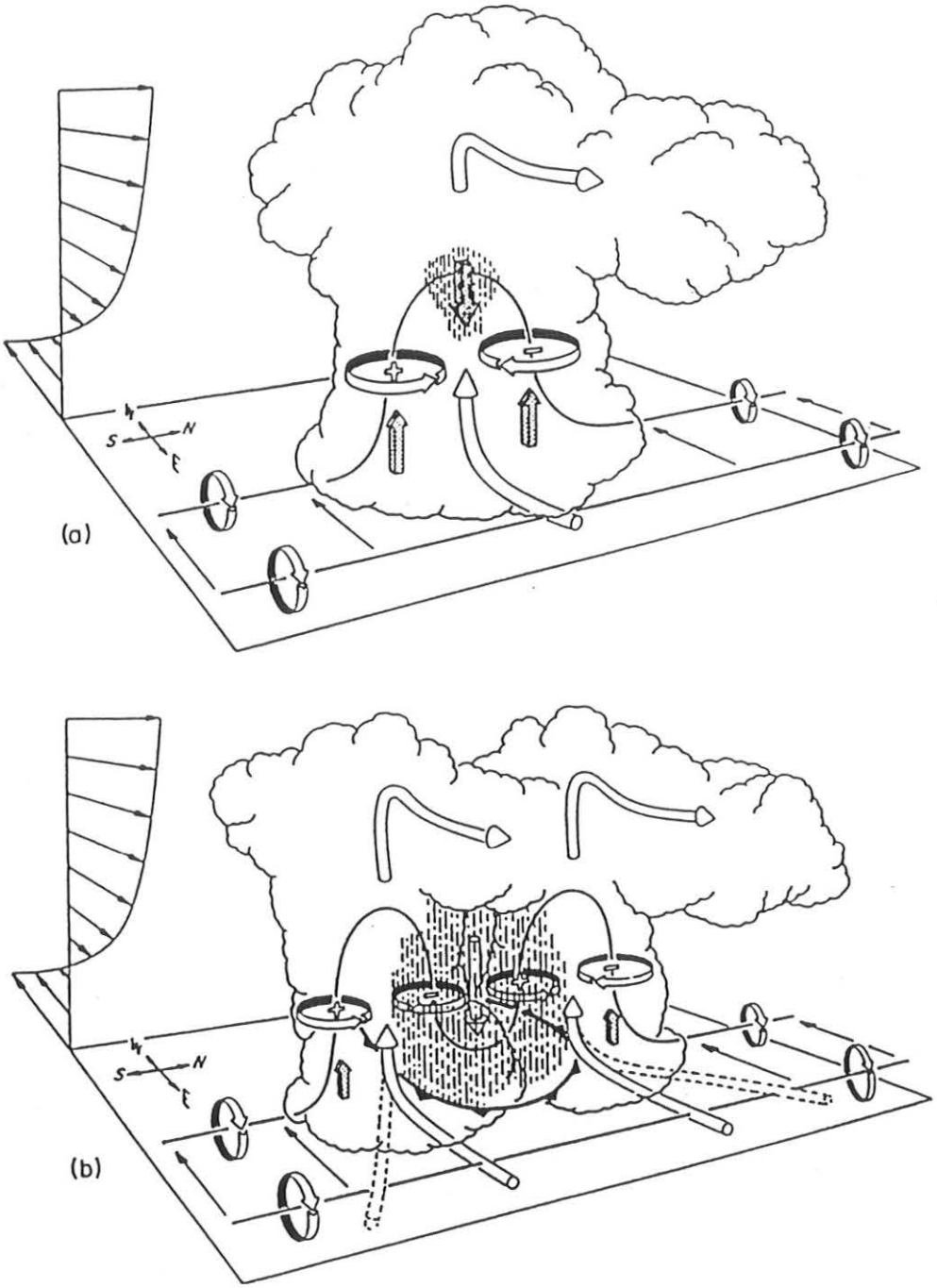

Figure 2 Depiction of how a vortex tube contained within westerly environmental shear is deformed as it interacts with a convective cell (viewed from the southeast). Cylindrical arrows show the direction of cloud-relative airflow, and bold solid lines represent vortex lines with the sense of rotation indicated by circular arrows. Shaded arrows show the forcing influences that promote new updraft and downdraft growth. Vertical dashed lines represent regions of precipitation. (a) Initial stage: Vortex tube loops into the vertical as it is pulled into the updraft. (b) Splitting stage: Downdraft forming between the splitting updraft cells tilts the vortex tubes downward, resulting in two vortex pairs. The barbed line at the surface marks the boundary of the cold air spreading out beneath the storm. (Adapted from Rotuno 1981)

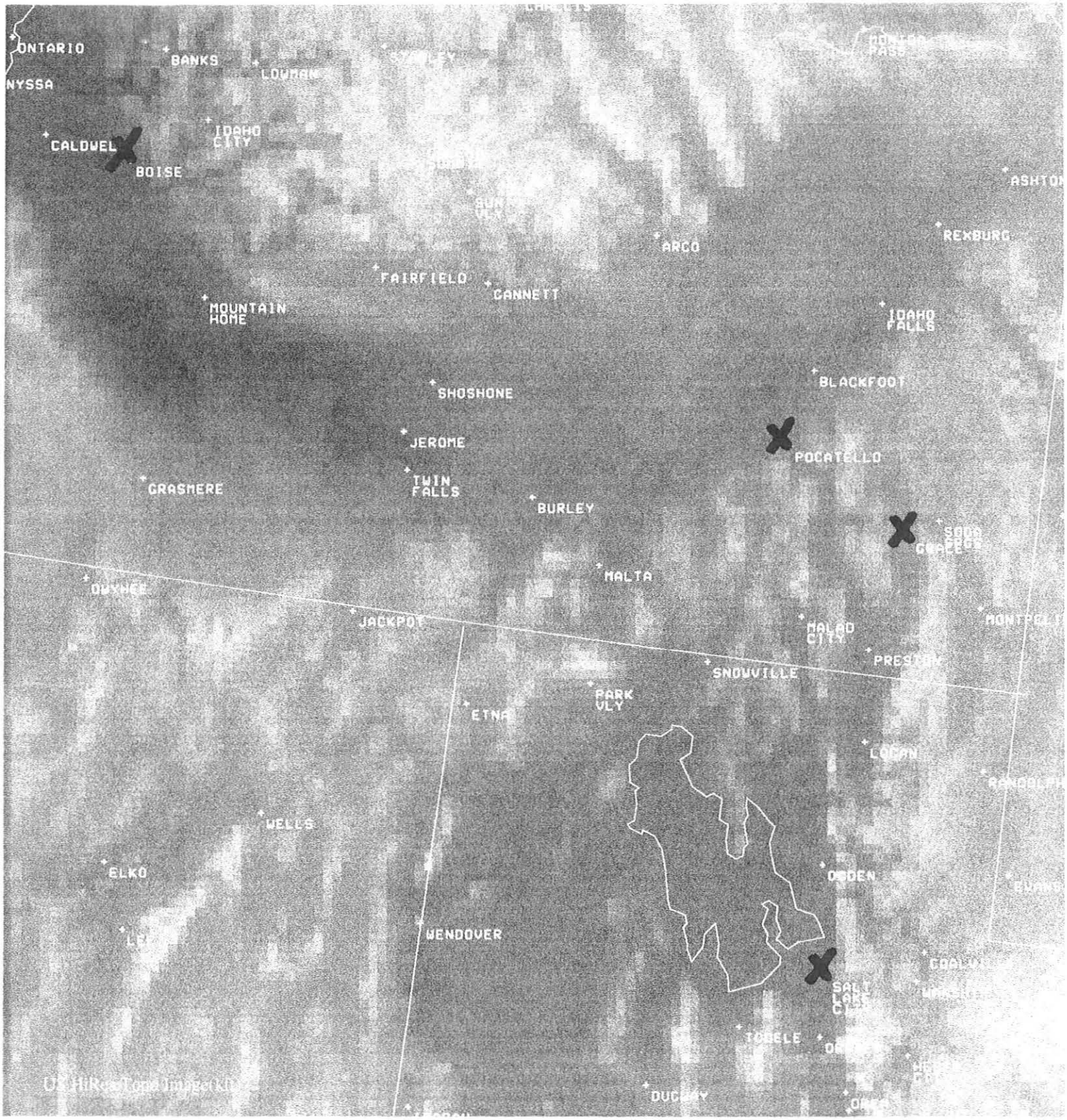

Figure 3 Topographical image of southern Idaho, northern Utah and northeast Nevada. **X** marks locations referred to in text.

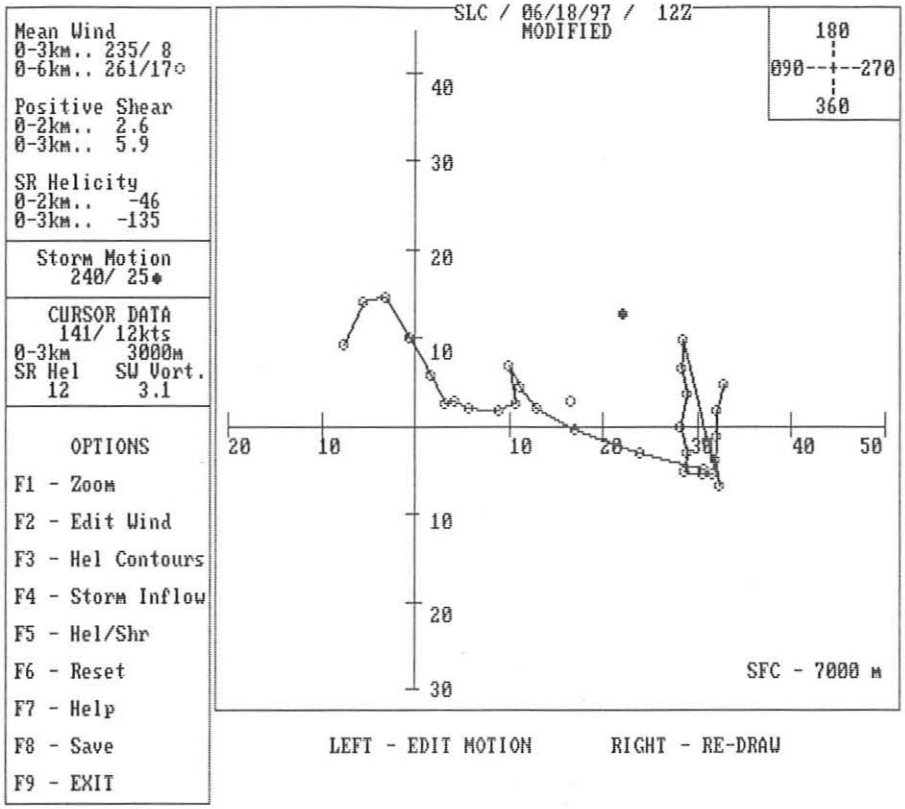

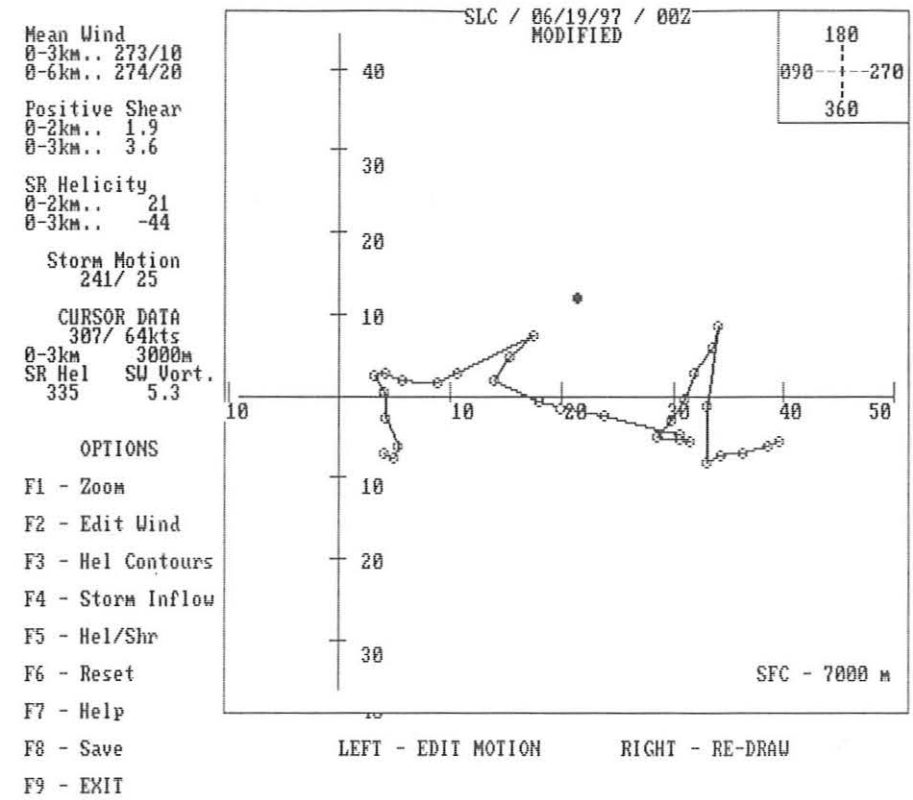

Figure 4 a) Hodograph from Salt Lake City sounding, 1200 UTC 18 June 1997. b) Hodograph from Salt Lake City sounding, 0000 UTC 19 June 1997. Note that the low-level winds in the vicinity of the splitting cells were likely southwesterly which would result in a hodograph that exhibited more unidirectional shear near the surface.

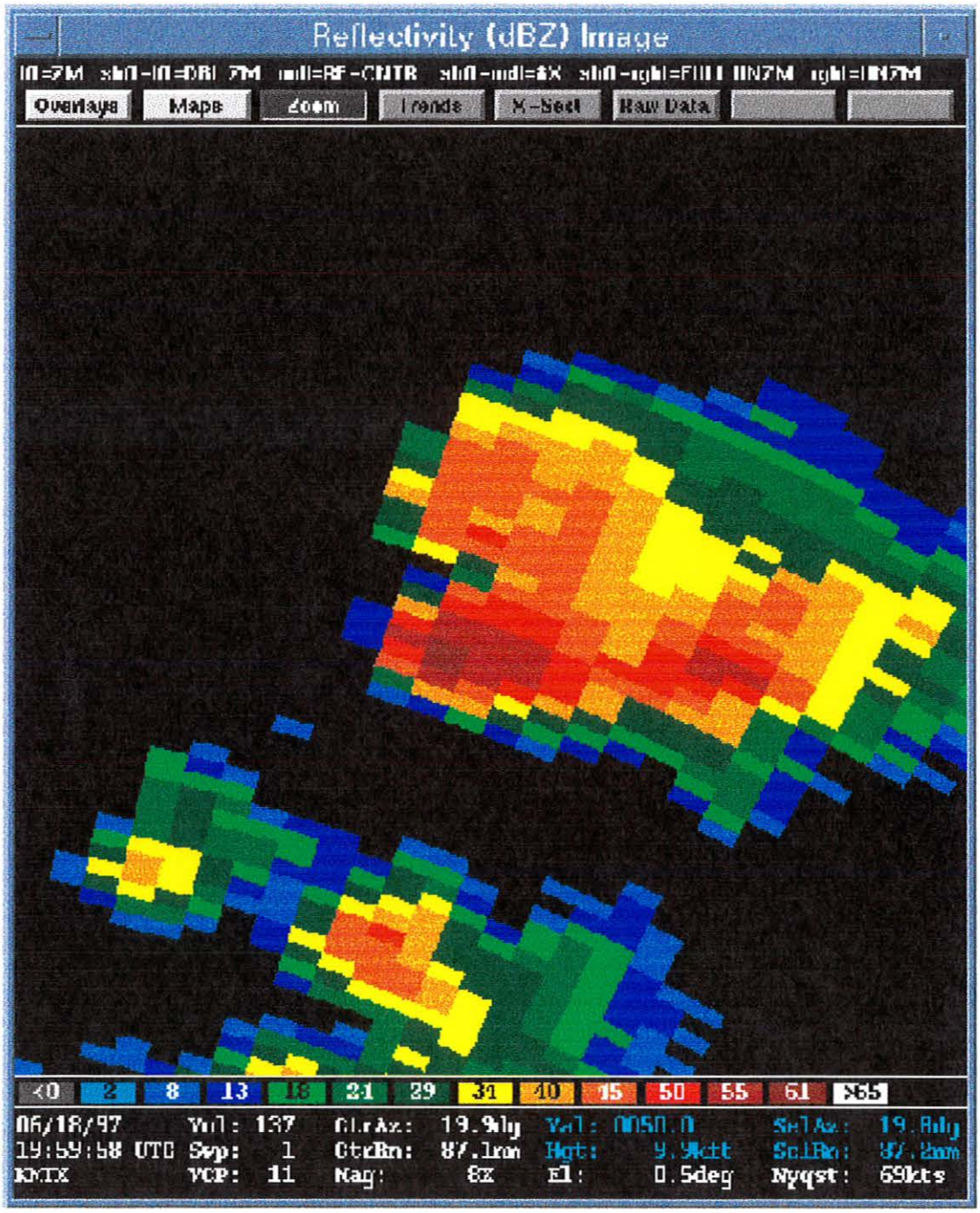

Figure 5 Base Reflectivity from the 0.5 degree elevation scan of the Salt Lake City area WSR-88D (KMTX), 1959 UTC 18 June 1997.

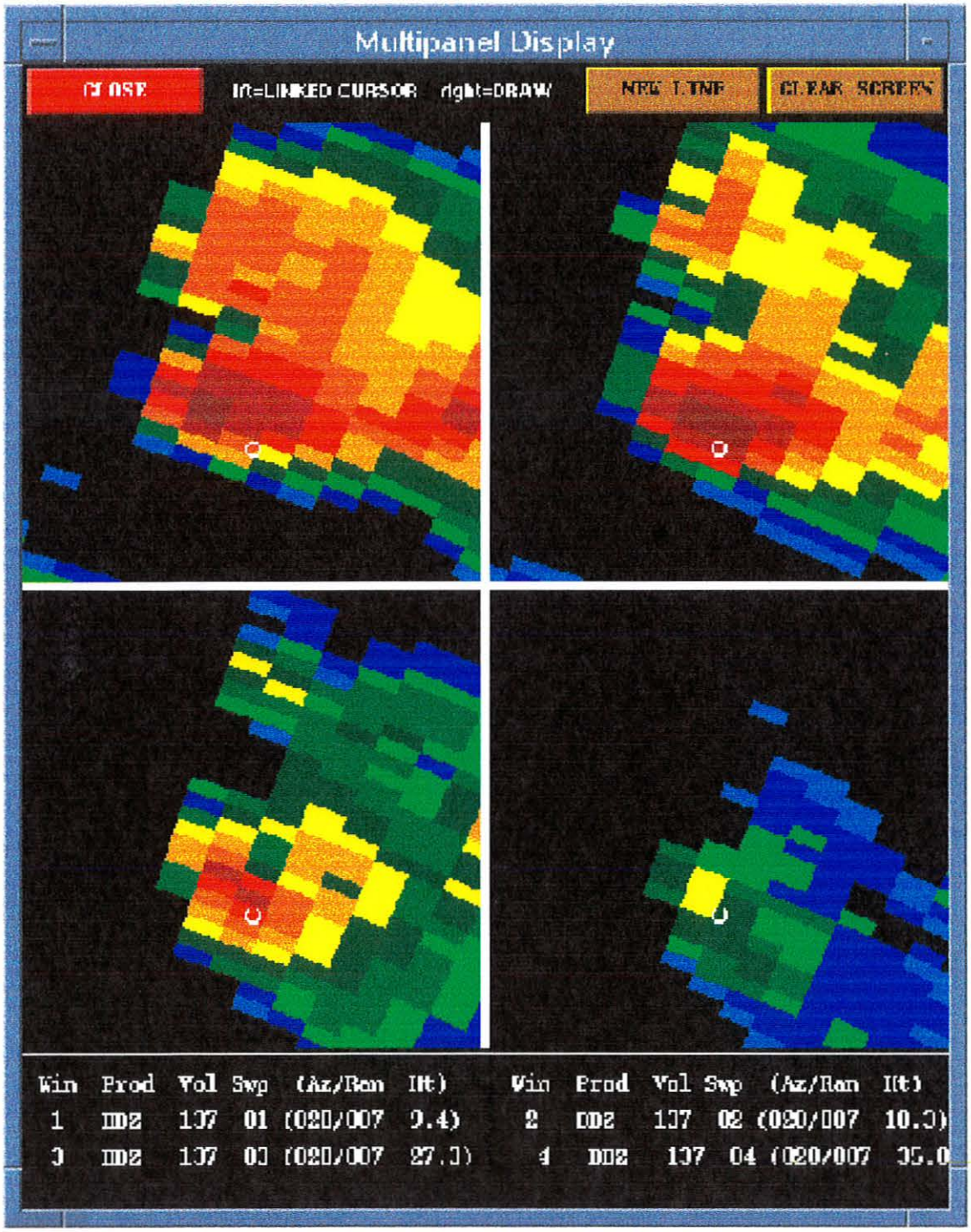

Figure 6 4-Panel of Base Reflectivity (0.5, 1.5, 2.4, and 3.4 degree elevation scans) from the KMTX WSR-88D, 1959 UTC 18 June 1997. Small white circle is placed along the tight low-level reflectivity gradient in quadrant 1 (upper left). Note the mid-level overhang in quadrant 3 (lower left) and the storm top (small yellow area) in quadrant 4 (lower right) which is shifted over the low-level reflectivity gradient.

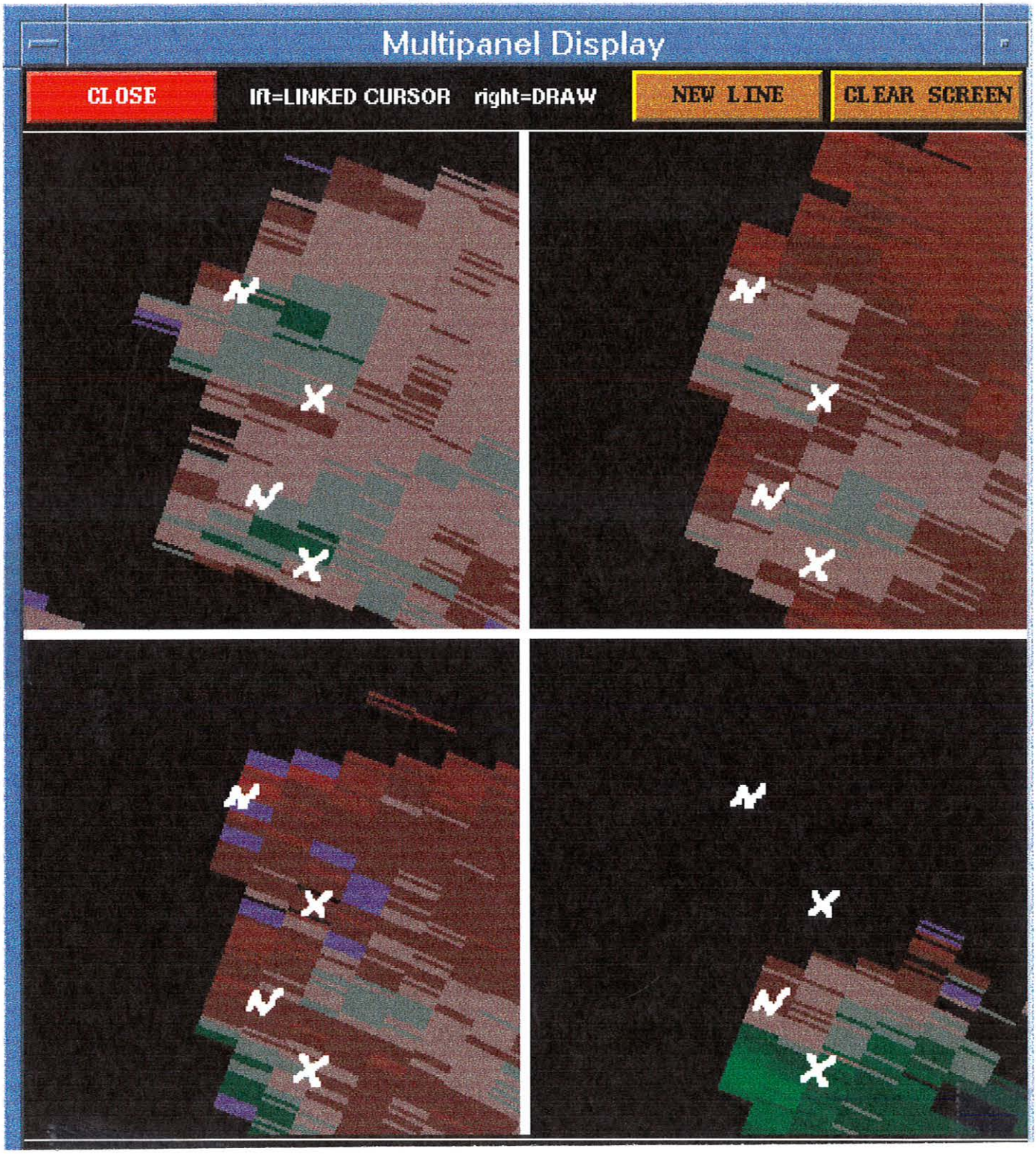

Figure 7 Storm Relative Velocity from the 0.5 degree elevation scan of the KMTX WSR-88d, 2004 UTC 18 June 1997. **X** marks the locations of apparent cyclonic rotation. **N** marks the location of apparent anti-cyclonic rotation.

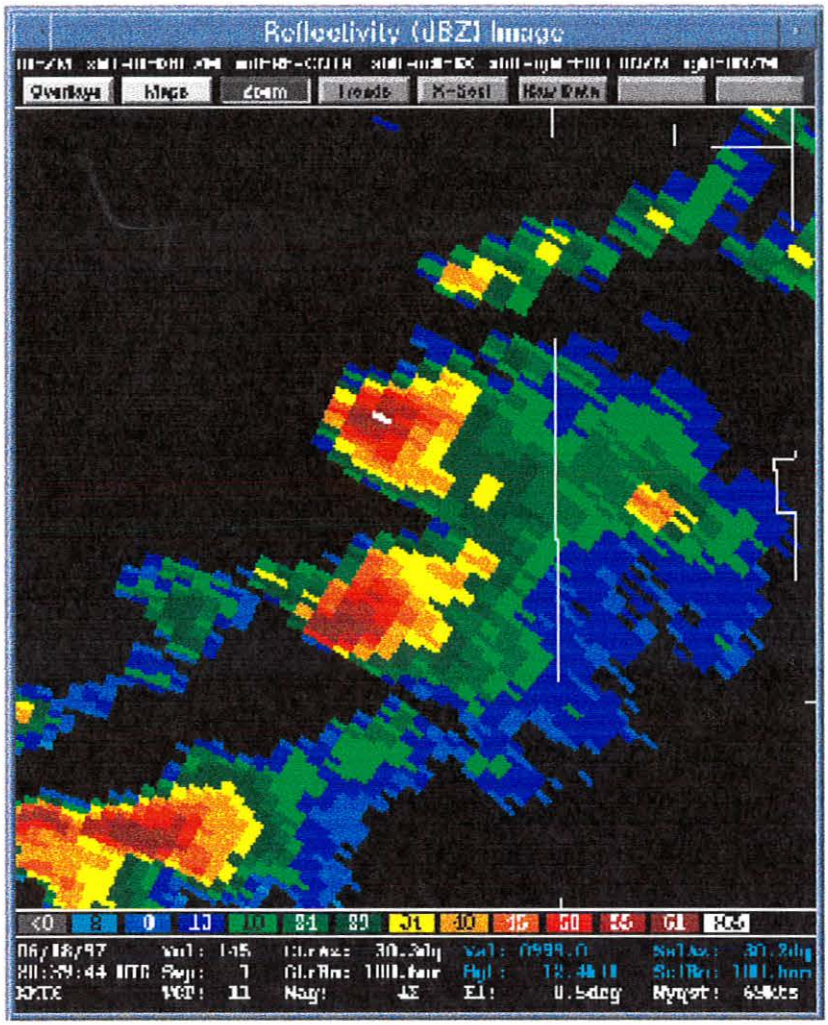

Figure 8 Base Reflectivity from the 0.5 degree elevation scan of the KMTX WSR-88D, 2039 UTC 18 June 1997. Note how the left moving cell (top) was accelerating out ahead of the right moving cell.